AUBE '01

12TH INTERNATIONAL
CONFERENCE ON AUTOMATIC FIRE DETECTION

March 25 - 28, 2001
National Institute Of Standards and Technology
Gaithersburg, Maryland U.S.A.

PROCEEDINGS

Editors: Kellie Beall, William Grosshandler and Heinz Luck

NIST CENTENNIAL 1901-2001

NIST
National Institute of Standards and Technology
TechnologyAdministration, U.S Department of Commerce

Darryl W. Weinert* and George W. Mulholland

Building and Fire Research Laboratory, National Institute of Standards and Technology, Gaithersburg, MD 20899, USA

*Guest Researcher on leave from the Center for Environmental Safety and Risk Engineering, Victoria University, Melbourne, PO Box 14428, VIC 8001, AUSTRALIA

An apparatus for light scattering studies of smoke particles

1. Introduction

There is great interest in being able to distinguish between flaming, non-flaming and nuisance alarm aerosols using light scattering methods. Commercially available light scattering smoke detectors are not able to make such distinctions. Past studies have examined various aspects of light scattering from smoke and nuisance aerosols. Two such studies [1] have examined the light scattering from smoke generated by flaming and non-flaming fuels using fixed position detectors. Loepfe et al. [2] made use of polystyrene spheres for calibration of their instrument and both studies had the instruments installed in a fire test room. Meacham and Motevaili [1] examined the detector response signals at individual angles, while Loepfe et al. **[2]** discriminated between smokes using the degree of linear polarization as a function of angle. We have developed a facility for measuring the light scattered by smokes as a function of the scattering angle and linear polarization. By using monosize polystyrene calibration particles and filter collection for gravimeteric measurement, we were able to measure for the first time the differential (angular distribution) scattering cross section per mass of a smoke aerosol. This differential mass scattering cross section is a measure of the light scattering strength of a particle in units of area per mass.

In this paper we focus on the optical design of the light scattering facility, the calibration method and results for acetylene soot. This method is applied to two non-flame generated smokes and three flame generated smokes and presented in another paper [3].

2. Apparatus

This study was carried out by adapting the existing large agglomerate optical facility (LAOF) developed at the National Institute of Standards and Technology (NIST), MD, USA. The LAOF was originally [4] used to measure the mass specific extinction coefficient for flame generated smoke and the total scattering coefficient using a reciprocal nephelometer [5], which has a cosine sensor/photomultiplier tube set at the center of the upper cell in Figure 1. For the differential light scattering experiments the long upper glass section with the tapered inlet was replaced with a short column. This column has opposing inlets on either side of the column to promote mixing of the aerosol when it

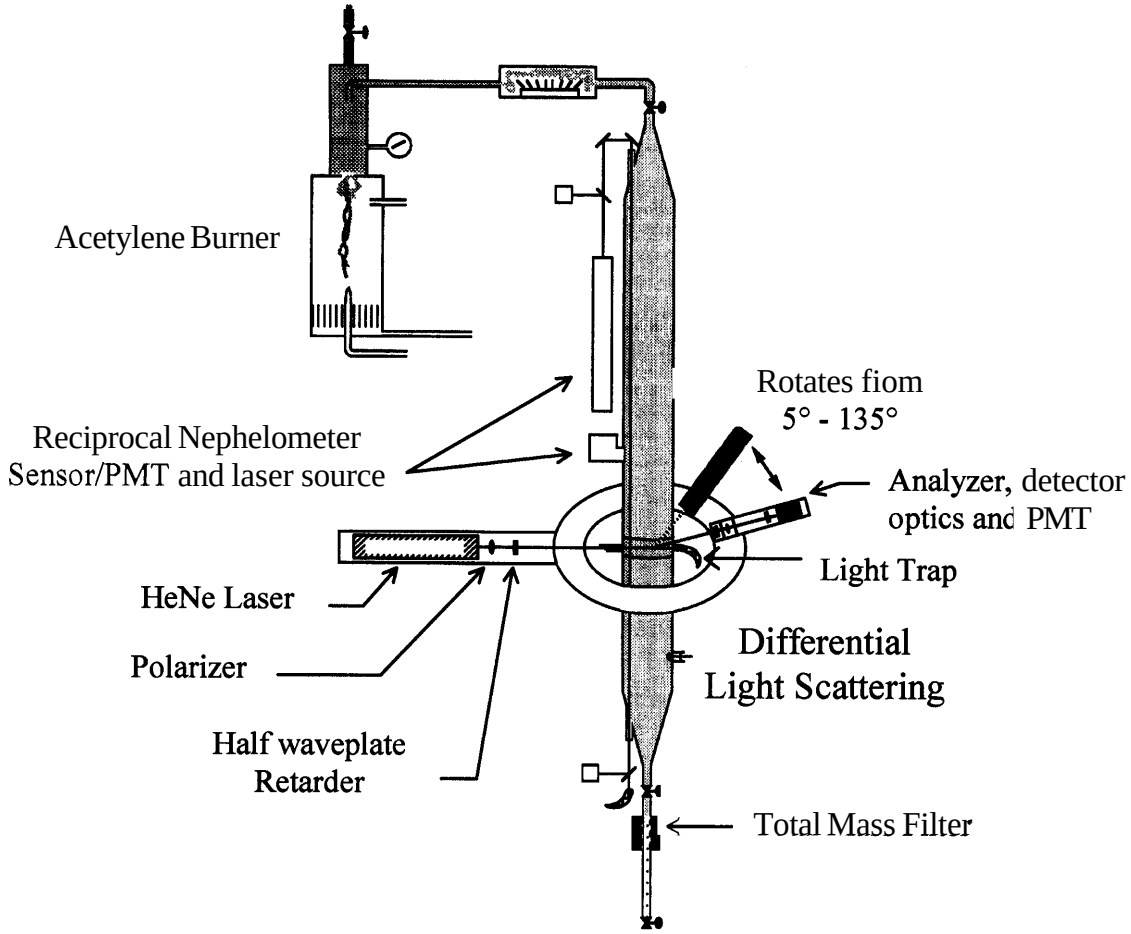

Figure 1: A schematic of the basic LAOF set up.

enters the LAOF. The particles are carried by the air flow to the scattering cell in the midsection of the column where the light scattering occurs. The particles then flow to the bottom of the LAOF where they are collected on a 47 mm filter at a known

volumetric flow rate. The mass concentration of the aerosol is determined from the mass of particles on the filter and the volume flow rate. A constant flow rate of 10 L min^{-1} is maintained with a mass flow controller followed by a vacuum pump.

3. Generation of Calibration and Smoke Aerosol

Nebulizing a suspension of monosize (nominally) **496** nm diameter **PS** spheres in water produces a monosize polystyrene latex **(PS)** aerosol which was used as the calibration aerosol. This size was chose for its similarity to non-flaming smoke particle sizes and its Mie scattering pattern, which is free of high frequency variation. The suspension is prepared by adding about **2** ml of the concentrated (0.0 1 volume fraction) suspension to 50 ml of particle free water. Nebulized droplets containing a single sphere evaporate **as** they flow through a diffusion drier, resulting in a **PS** aerosol. The drier consists of a 500 mm long, **70** mm ID tube with a 10 mm diameter screen tubing surrounded by silica gel. A majority of the particles are singlets but there is a small fraction of doublets resulting from the drying of a droplet containing two spheres. Once the spheres have exited the diffusion drier some dilution air is added to the flow at a rate of about **5** L min^{-1} and this aerosol stream is passed into a 3 L volume for final mixing. The flow is then introduced into the LAOF. A by-pass exists between the mixing volume and the LAOF to maintain nearly atmospheric pressure in the LAOF. A filter is connected to the by-pass line to prevent **PS** spheres from escaping into the atmosphere if the flow rate of **PS** aerosol should be greater than the vacuum flow rate. **Also** the by-pass filter will prevent ambient particles from entering the system if the **PS** aerosol flow rate is less than the vacuum flow rate.

The acetylene smoke used in this study was produced in a steady-state and repeatable manner by a co-flow laminar diffusion burner [6]. The smoke concentration was adjusted to the required range by adding dilution air to the small amount of soot that is sampled from the burner before it enters the scattering cell.

4. Optical System

The light scattering cell is located in the midsection of the LAOF and fabricated from 10 cm inner diameter glass tubing ending in ground glass flanges. The flanges allow

connection to the upper and lower neighbors, which are also fabricated from glass. The scattering cell has an entrance window for the incident light beam and a light trap directly opposite. The scattering plane is defined to be the plane in which the incident and scattered beams lie; for our experiments this is the horizontal plane. The scattering angle, θ, is given by the angle measured from the direction of propagation, so that $\theta = 0°$ is the forward direction of the incident beam. The incident beam originates from a HeNe laser (wavelength $\lambda = 632.8$ nm) in continuous wave (CW) mode which has a 500:1 linear polarization ratio. The CW beam is immediately passed through a rotating chopper ($f = 80$ Hz) to reduce background noise when measuring low signals. The incident beam then passes through an optical train of polarizing elements that prepare the optical properties of the beam. This optical train consists of a linear Glan-Taylor type generating polarizer orientated with its optical axis at an angle $\phi_P = 0°$, where ϕ_P is the angle of the optical axis of the polarizer from the scattering plane. A subscript H then is then used to denote this polarization as the horizontal polarization. This generated polarization essentially eliminates the residual perpendicular or vertical (subscript V) polarization of the laser. The next optical element is a quartz zero-order half-waveplate retarder. This is the key element in the incident optical train as a 45° rotation of its fast axis from the scattering plane induces a rotation of the beam from horizontal to vertically polarized light. In this way an incident polarization of either horizontal or vertical orientation can be chosen. The next optical element before the scattering volume is the entrance window, which is set at a slight angle to avoid the multiple reflection of the incident beam. This angle does have an effect of reducing the intensity of the incident beam, as do all the other elements of the incident light optical train. After passing through the window, the laser beam passes through a 10 cm pathlength of uniformly distributed smoke or calibration aerosol. The light scattering is apparent as a red line of light with a few bright spots arising from large agglomerate particles in the case of the acetylene smoke.

The scattered light first passed through the wall of the LAOF's scattering cell with a slight loss of light due to reflection. The opposite side of the scattering cell to the detectors view was coated in a base layer of matte black paint and then a layer of carbon

paint was added onto this. Reducing reflection of scattered light entering the detector field of view. This was particularly important near the entrance window and the light trap as reflections and stray light were appreciable in these areas. The entrance window itself had to be kept to a small diameter, so that plasma light from the laser and beam dispersion did not create a large area of reflection bigger than the entrance of the light trap, which was 5 mm. The effect of this stray light at the entrance window and near the light trap entrance would otherwise add significantly to the scattered light signal in the forward and 135° directions respectively.

To align the polarizers optical axes correctly, the first generating polarizer is set in a precision mount and reference to a polarizing beam splitter. A null or crossed polarizer approach is then used to determine the positions for the half waveplate and the analyzer, so that horizontal incident and horizontal scattered polarized light (HH) can be produced and similarly, vertical-vertical polarization (VV). The analyzer is a linear polarizer used to measure the vertical or horizontal scattered light incident on the detector. The generating polarizer was set at either $\phi_P = 90°$ or $\phi_P = 0$ to cross the analyzer during alignment, but was not changed from the $\phi_P = 0°$ position during an experiment. Once the polarizer and analyzer were aligned, the half waveplate retarder was placed in the optical train and aligned. The analyzer, ϕ_A, and retarder, ϕ_R, angles are changed manually as required when conducting an experiment. These changes were found to cause a standard uncertainty of about 3 % (1 std. deviation) in the measured signal. In this paper the standard uncertainty refers to one standard deviation about the mean value of a series of measurements. The combined uncertainty refers to the combined standard uncertainties of the variables using a root-sum-of-squares method. All uncertainties are expressed as a percentage of the mean value.

The scattered light was detected by a series of optical elements mounted on a rotation stage with stepper motor drive and encoder feedback. PC control of the rotation stage was accomplished by a computer program and interfaced through an indexer-board in the PC. This program also monitored the detector signal via an analogue-to-digital converter board. The rotation stage would move the detector and its optical elements in

A $\theta = 5°$ steps in the scattering plane from $5°$ to $135°$ to measure the scattered light. Essentially any angle in the range could be chosen for a measurement; for example, an extra measurement is usually made at $\theta = 8°$. Alignment of the detector zero position was also automated but required the placement of neutral density filters in the incident beam and removal of the light trap. The rotation stage was then positioned manually until the detector indicated a peak intensity was found. The computer program then made the rotation stage scan a range of $\pm 2.5°$ about this peak position in 0.25" steps. The peak signal detected was then redefined as zero and another fine step scan was conducted from $\pm 1°$ of this position in 0.1" steps; again the peak position was redefined if necessary and this became the $\theta = 0°$ position. The detector would then move out of the beam to the 4" resting position to await the beginning of an experimental scan.

The first optical element carried by the detector rotation stage was the analyzing polarizer, a Glan-Taylor prism, which was aligned to analyze either the horizontal, $\phi_A = 0°$, or vertical polarization, $\phi_A = 90$" component of the scattered light for a given scan. Following the analyzer was a 5 mm entrance aperture of the detector housing. The detector housing is a sealed tube containing (in order) a laser line filter, an achromatic lens, a 1 mm diameter aperture stop, a diffuser and finally the side mounted photomultiplier tube. The filter reduces the background by allowing only the laser wavelength to pass. The achromatic lens with the aperture at the focal point of the lens is positioned to limit the scattered light to $\pm 0.3°$ of the scattering angle. This small acceptance angle is important for minimizing the forward scattering bias at small angles. A large area diffuser is positioned between the aperture stop and PMT to spread the initially focused beam over the active area of the PMT and reduce the effects of PMT polarization dependence.

The signal from the PMT was taken through a variable resister to a lock-in amplifier unit. The lock-in used a chopper to provide the lock-in frequency and the sensitivity of the amplifier was chosen manually when required as the detector is moved to a new position. The output signal from the lock-in was then passed through a voltage divider to the analogue-to-digital converter in the controlling PC. In a series of calibration and

smoke experiments the sensitivity of the amplifier is the only parameter in the detection circuit that is changed.

As the detector scans through the scattering angles, the scattering volume changes in proportion to $1/\sin(\theta)$. This angular dependence results in more than a factor of 10 change in the detector's view of the scattering volume as the scattering angle increases from 5° to 90''. To correct for the effects of angular dependence of the scattering volume geometry as well as signal scaling, a calibration needs to be performed.

5. Calibration

By scattering light from the **PS** calibration aerosol and then normalizing the detected signal by the theoretical signal for theses spheres we can determine a calibration function, $K(\theta)$. This calibration function corrects for the scattering volume, detector effects, and the small error effects of the optical train. In this study the calibration function also includes the scaling due to the incident beam irradiance, as we have assumed that it is constant during the experiments. The object of these calibrations is to determine the differential (angular distribution) **mass** scattering cross section, $\sigma(\theta)$, of the smoke particles to be examined.

From Debey-Mie theory **[7]** the differential scattering cross section, $C_{th}(\theta)$, for a single **496** nm polystyrene sphere is calculated. This is then converted to a theoretical differential scattering cross section per **mass,**

$$\sigma_{th}(\theta) = C_{th}(\theta)/V_p\rho_p\,, \qquad (1)$$

by dividing by the particles **mass;** here the values V_p and ρ_p are the particle volume and density (1.05 g $\mathbf{cm^{-3}}$ for **PS** spheres) respectively. The calibration experiment is conducted by introducing the **PS** spheres into the scattering volume and making detector signal measurements, $U_p(\theta)$, for a given polarization. The detector signal, $U_p(\theta)$, has a dependence on the scattering volume that varies as $1/\sin(\theta)$ to the first order, this can be corrected by calculating $u_p(\theta) = U_p(\theta)\sin(\theta)$. The **mass** concentration, M_p, of calibration particles is determined from the filter **mass.** The theoretical value, $\sigma_{th}(\mathbf{0})$, is

used to normalize the detector signal to determine the calibration function, $K(\theta)$, such that

$$K(\theta) = \frac{u_p(\theta)}{M_p \sigma_{th}(\theta)} \tag{2}$$

where p is the subscript for the calibration particle values. The calibration function is

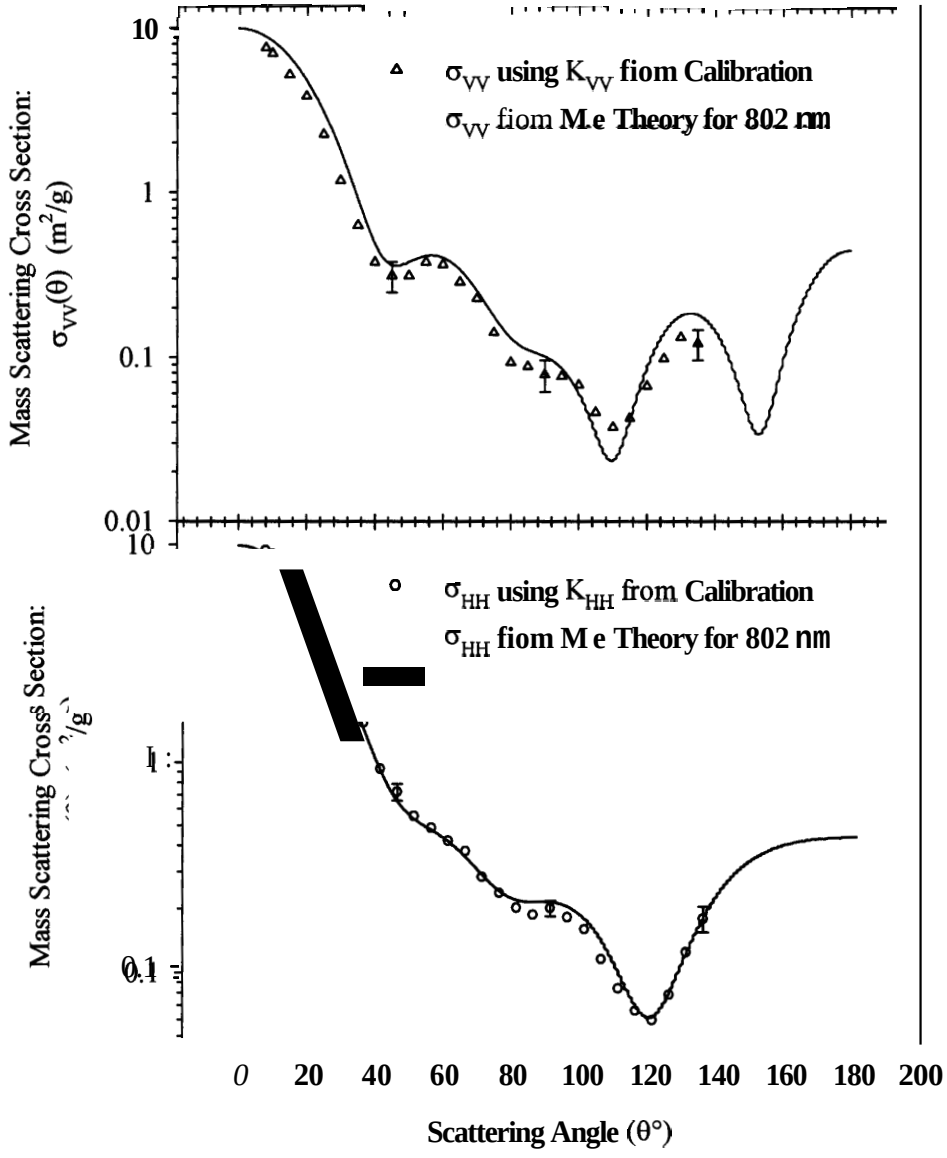

Figure 2: Light scattering results, VV and HH polarization, for nominally 802 nm diameter PS spheres.

determined from **Eq.** (2), for each angle of measurement and for two different polarization states: incident and detected vertical, $K_{VV}(\theta)$ **,** and incident and detected horizontal polarization, $K_{HH}(\theta)$. The angular average, K_{VV} and K_{HH} **,** of the calibration function is then determined and referred to as the calibration factor. Averaging reduced overcompensation caused by using the respective calibration functions, which weighted minima in the calibration particles scattering cross section too strongly. When an experiment with an aerosol is conducted both the volume corrected detector signal, $u(\theta)$, and the **mass** concentration of particles, M, are determined to then give the particles **mass** scattering cross section for a given polarization (polarization notation suppressed),

$$\sigma(\theta) = \frac{u(\theta)}{M K}. \tag{3}$$

The calibration factor would be determined from calibration experiments directly preceding an aerosol experiment.

In Figure **2** the application of an average calibration factor to the scattering signal from **802** nm nominal diameter **PS** spheres has been shown. The difference between experiment and theory is about **20** % of the Mie theory for $\sigma_{VV}(\theta)$ and less than about 10 % for $\sigma_{HH}(8)$. The larger deviation in $\sigma_{VV}(\theta)$ is due to a **miss** alignment of the optical elements in this case, but the agreement between the data sets is still quite clear. Error bars are shown for sample points only, and indicate combined uncertainty of a measurement when considering the variables of Eq. **2** and 3. The largest component of this combined uncertainty is due to the use of the angular average of the calibration function, which have standard uncertainty typically about 10 % in the HH polarization and 15 % in the VV polarization. The standard uncertainty of a detector signal measurement, of which 10 are made at given angle in an experiment, varies between **2** % and **6** %, approaching the higher value for smaller scattering signals. Specific effects due to doublets of polystyrene sphere are unknown for our experiments.

6. Smoke Results

Before each set of **VV** and HH measurement of the light scattered from smoke particles,

a set of calibration experiments would be completed. The calibration factor from these experiments would then be applied to the detector signal for the smoke particle experiments that followed. **A** second set of calibration experiments was completed after the smoke to ensure that no change in system calibration had occurred. Figure **3** shows the first measurement of the mass scattering cross section for acetylene from a laminar co-flow diffusion burner, the general shape of the data curve is consistent with that reported by others [8]. However, our results go beyond previous studies by including the cross section per mass concentration. Such information is important in comparing measurement and theory. The repeatability of the measurements is demonstrated by the presence of a second experiment's results. The minima at $\sigma_{HH}(90)$ is a result of Rayleigh-like scattering of the small primary particles that make up the agglomerate.

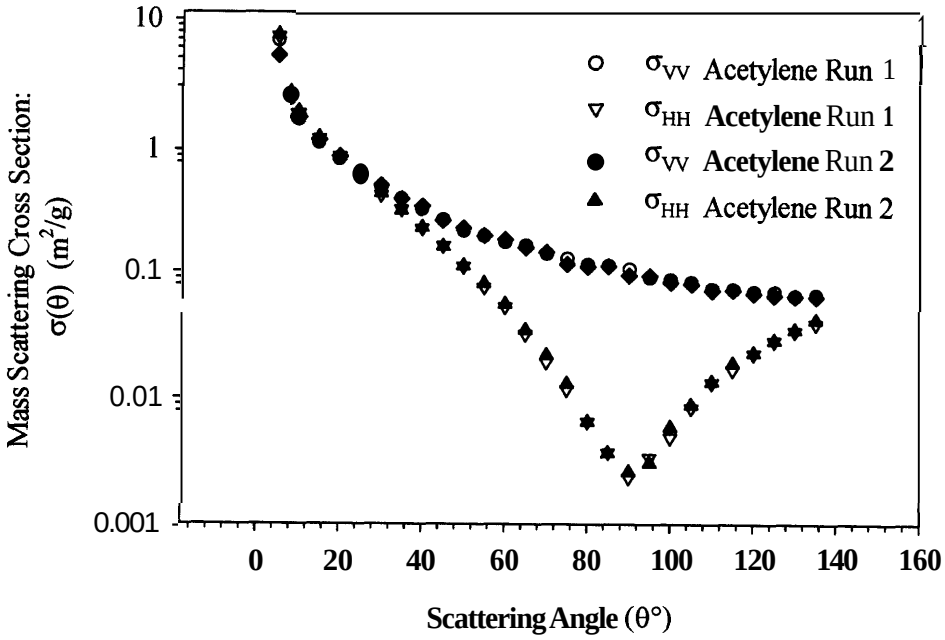

Figure 3: Differential **mass** scattering cross section results for acetylene soot.

The influence of the far field interference between the light scattered by individual primary particles in the soot agglomerate is apparent at the forward scattering angles, and the **2** to 4 order of magnitude changes in the scattering cross sections over the

angular range. The light scattered by the soot agglomerate is related to the morphology of the soot agglomerate and thus its fractal geometry [6].

With the differential mass scattering cross section determined it is then possible to determine the truncated (5° to 135°) total **mass** scattering cross section, C_{msca} , of the particles, which is given by:

$$C_{msca} = 2\pi \int_{5}^{135} \frac{(\sigma_{VV}(\theta) + \sigma_{HH}(\theta))}{2} \sin(\theta) d\theta \,. \qquad (4)$$

The integration was performed numerically and calculated cross sections are shown in Table 1. The results are also compared to Debye-Mie theory and results from other studies.

Particles	Total Mass Scattering Cross Section (m^2/g)	Uncertainty (m^2/g)
Mie Theory for **802** nm diameter	**7.49**	
802 nm diameter PS Spheres	**6.3, 6.1**	± **1.6**
Acetylene Soot*	**1.95**	±0.08
Acetylene Soot	**1.8, 2.0**	±**0.5**

Table 2: Truncated total mass scattering cross sections for the particles investigated in this study. The results for our multiple experiments (Runs 1 **& 2)** are shown. *This result is a measured total quantity, not truncated [4].

7. Conclusion

This study has demonstrated the application of polystyrene spheres suspended in air as a calibration technique for measurements of the differential scattering cross section per **mass,** $\sigma(\theta)$. Introduced for the first time was the quantification of aerosol particle scattering in terms of the differential scattering cross section per mass, which is made possible by gravimetric measurement of the particle mass concentration. This will allow direct comparison between measurements and light scattering theory. The light scattering apparatus used in these measurements has provided repeatable results over a

dynamic signal range of **3** to **4** orders of magnitude. Uncertainties lie in the range of 10% to **20%** and are mainly due to the uncertainties in the calibration factor. The method was then applied to acetylene smoke, which was produced in a consistent and reproducible manner by a co-flow laminar diffusion burner, facilitating the experimental measurements.

Reference List

[1] Meacham BJ, Motevalli V: Characterization of smoke from smoldering combustion for the evaluation of light scattering type smoke detector response. ***Journal of Fire Protection Engineering*** **1992;** ***4:*** **17-28**

[2] Loepfe M, Ryser P, Tomkin C, Wieser D: Optical properties of fires and non-fire aerosols. ***Fire Safety Journal*** **1997; 29: 185-194**

[3] Weinert DW, Cleary T, Mulholland GW. Size distribution and light scattering properties of test smokes. ***Submitted: A UBE 2001***

[4] Mulholland, G. W. and Choi, M. ***Y.*** Measurement of the mass specific extinction coefficient for acetylene and ethylene smoke using the large agglomerate optics facility. The Combustion Institute. Twenty-Seventh Symposium (international) on Combustion. **1515-1522. 1998.** Pittsburgh, The Combustion Institute.

[5] Mulholland GW, Bryner NP: Radiometric model of the transmission cell-reciprocal nephelometer. ***Atmospheric Environment*** **1994; 28:873-887**

[6] Samson **RJ,** Mulholland GW, Gentry J W Structural analysis of soot agglomerates. ***Langmuir*** **1987;** 3:272-281

[7] Bohren CF, Huffman D R ***Absorption and scattering of light by small particles*** New York, John Wiley & Sons, **1983**

[8] Koylu UO, Faeth GM: Optical properties of overfine soot in buoyant turbulent diffusion flames at long residence times. ***Journal of Heat Transfer*** **1994;** 116:152-159